



# CHORUS

This is the accepted manuscript made available via CHORUS. The article has been published as:

## Vacant-Site Octahedral Tilings on SrTiO<sub>3</sub> (001), the $(\sqrt{13} \times \sqrt{13})R33.7^\circ$ Surface, and Related Structures

D. M. Kienzle, A. E. Becerra-Toledo, and L. D. Marks

Phys. Rev. Lett. **106**, 176102 — Published 29 April 2011

DOI: [10.1103/PhysRevLett.106.176102](https://doi.org/10.1103/PhysRevLett.106.176102)

# **Vacant-site Octahedral Tilings on SrTiO<sub>3</sub> (001), the ( $\sqrt{13}\times\sqrt{13}$ )R33.7° Surface and Related Structures**

D. M. Kienzle, A. E. Becerra-Toledo, L. D. Marks

Department of Materials Science and Engineering, Northwestern University, 2220 Campus Drive,  
Evanston, Illinois 60208, USA

The structure of the SrTiO<sub>3</sub> (001) ( $\sqrt{13}\times\sqrt{13}$ )R33.7° surface reconstruction has been determined using transmission electron diffraction combined with direct methods and density functional theory. It has a TiO<sub>2</sub>-rich surface with a 2D tiling of edge or corner-sharing TiO<sub>5</sub>□ octahedra. By tiling these units and forming network surface structures dictated by local bond valence sums, many ordered surface reconstructions can be generated as well as disordered glass-like structures consistent with the multitude of structures observed experimentally, and potentially other materials and interfaces.

PACS: 68.35.Bt, 68.37.Lp, 68.35.Md

Strontium titanate is the archetypal perovskite, and if we can understand its surface structure much can be deduced about the surfaces of similar perovskite materials important for numerous applications in areas of thin film growth and catalysis. A bewildering large number of different reconstructions have been experimentally observed on the SrTiO<sub>3</sub> surface including a series of ( $n \times n$ ) reconstructions on the (111) surface [1], ( $n \times 1$ ) and ( $1 \times n$ ) reconstructions on the (110) surface [2] and an even larger number for the (001), namely, the ( $1 \times 1$ ) [3-10], ( $2 \times 1$ ) [4,8,9,11-13], ( $2 \times 2$ ) [8-10,14-16],  $c(4 \times 2)$  [11,14,17,18],  $c(4 \times 4)$  [4,8,16], ( $4 \times 4$ ) [16],  $c(6 \times 2)$  [11,12,17-19], ( $6 \times 2$ ) [18],  $(\sqrt{5} \times \sqrt{5})R26.6^\circ$  [16,20-23],  $(\sqrt{13} \times \sqrt{13})R33.7^\circ$  [12,16] (RT13 hereafter) plus many more [24] which may only be locally stable such as a  $(4\sqrt{2} \times \sqrt{2})R45^\circ$ .

It is now established that many of these are based on a TiO<sub>2</sub> double-layer with units of TiO<sub>6</sub> or TiO<sub>5</sub>□ (□ a vacant site). For others, either a single Sr adatom [16] or O vacancy [21] has been suggested from scanning tunneling microscopy (STM) images. However, there are many other ways one can obtain similar STM images so only considering two different structures is not a structure solution. In addition, via basic chemical reasoning a semi-naked Sr atom sitting on a surface is highly unlikely as Sr is much more basic than Ti.

For the (110) surface, once one structure of the ( $n \times 1$ ) family of reconstructions was solved [2] it was possible to deduce others, a conclusion supported by STM images and density functional theory (DFT) calculations. The key was recognizing that they could all be described as rings of TiO<sub>4</sub> tetrahedral units with different packings leading to different valence-neutral unit cells. This letter presents a structural solution of the RT13 (001) reconstruction using transmission electron microscopy (TEM) supported by relatively high-level DFT calculations. Similar to the (110) surface, this is a valence-neutral surface, but with TiO<sub>5</sub>□ in a more open structure as dictated by the topology of the underlying bulk structure. We are also able to identify some other candidate valence-neutral surface structures with similar elements, such as the  $(\sqrt{5} \times \sqrt{5})R26.6^\circ$ . There are many others, all with relatively similar surface energies that could occur locally, consistent with the plethora of observed structures. These surfaces are best considered as 2D analogues of bulk SiO<sub>2</sub> glass, consistent with the original concept of network glasses proposed by Zachariasen [25] where one can have ordered and disordered structures all preserving local co-ordination and bond-valence sums [2]. Even with accounting for topological constraints of the underlying bulk structure as well as the requirement of valence neutrality, many

different, but fundamentally similar local structures can be obtained for both the (001) and (110) surfaces and presumably other perovskite surfaces, possibly including interfaces.

Single crystal SrTiO<sub>3</sub> (001) (99.95% purity) substrates were purchased from MTI Corporation (Richmond, CA) and conventionally prepared for TEM by cutting 3 mm-diameter discs, mechanically thinning each to 100 μm, dimpling the center to 20 μm, and ion-beam polishing with 4-5 keV Ar<sup>+</sup> ions to electron transparency. Samples were etched with a NH<sub>4</sub>F-HF solution (pH 5) for 45 seconds to preferentially remove SrO then annealed in a tube furnace with flowing oxygen (100 sccm) for 5 hours at 1050°C to produce the air stable RT13 reconstruction. As we will see, this preparation method led to surfaces with a lower TiO<sub>2</sub> excess thereby allowing us to access different reconstructions.

TEM images and off-zone diffraction patterns were taken before etching and after annealing with a Hitachi 8100 TEM operating at 200 kV. Diffraction patterns were recorded with film for a range of exposure times (2-90 seconds) and digitized with an Optronics P-1000 microdensitometer. Spot intensities from both domains were measured using a cross-correlation technique [26] and merged to create a single data set. The data set was reduced by *p4* plane-group symmetry to 43 independent beams. Direct methods (EDM 3.0) [27] were implemented to generate 2D scattering potential maps of possible surface structures.

DFT was used to obtain atomic positions in the out-of-plane direction that cannot be determined from the scattering potential map, as well as a way to check the validity of in-plane positions and calculate the energy of the surface. A 3D periodic surface slab model was created using the in-plane DFT optimized bulk lattice parameters and 7 layers of SrTiO<sub>3</sub> bulk (412 atoms) separated by 10 Å of vacuum. Atomic positions were optimized using the full-electron potential WIEN2k package [28] with an augmented plane wave + local orbitals (APW+lo) basis set, the PBEsol [29] generalized gradient approximation as well as the revTPSS method [30]. Similar to work for the NiO (111) surface [31], we optimized the exact-exchange parameter for the Ti-d levels using experimental energies of some TiO<sub>x</sub> molecules [32] which gave a result of 0.5. While this is not a panacea of all DFT ills, and the exact-exchange fraction is surprisingly large, this gave a noticeably better value of 1.36eV for the decomposition energy of SrTiO<sub>3</sub> to SrO and TiO<sub>2</sub> compared to previous work [32], a better band-gap of ~2.8(1) eV as well as a good absolute fit to the ratio of the surface free-energy of SrTiO<sub>3</sub> (001) to (110) from Wulff construction measurements [33], none of these being part of the fitting. Typical muffin-tin radii were 1.55, 1.75, and 2.36 Bohr for O, Ti, and Sr, respectively, a 1x1x1 *k*-point grid, and a plane wave cut-off of  $K_{\max} * \min(\text{RMT}) = 7.0$ . Other known (001) surface structures were calculated for

comparison with similar parameters, excepting the  $k$ -point sampling which was kept at the same inverse volume density. The surface energy per  $(1 \times 1)$  surface unit cell ( $E_{surf}$ ) was calculated as:  $E_{surf} = (E_{slab} - E_{STO} * N_{STO} - E_{TO} * N_{TO}) / (2 * N_{1 \times 1})$ , where  $E_{slab}$  is the total energy of the slab,  $E_{STO}$  the energy of bulk SrTiO<sub>3</sub>,  $N_{STO}$  the number of bulk SrTiO<sub>3</sub> unit cells,  $E_{TO}$  the energy of bulk rutile TiO<sub>2</sub>,  $N_{TO}$  the number of excess TiO<sub>2</sub> units, and  $(N_{1 \times 1})$  the number of  $(1 \times 1)$  surface cells. A reasonable estimation of 0.05 eV/ $(1 \times 1)$  cell was used for revTPSS DFT error.

Imaging RT13 samples show a well-ordered surface with faceting along the  $\langle 010 \rangle$  and  $\langle 100 \rangle$  directions indicative of a TiO<sub>2</sub>-terminated surface [34], as expected when using a BHF etchant (see supplemental material). FIG 1 shows a typical off-zone diffraction pattern, with the two domains of the RT13 marked in addition to the bulk  $(1 \times 1)$  cell. The RT13 reconstruction was observed in areas of several microns squared and never in the presence of another reconstruction.

An EDM analysis resulted in only one feasible scattering potential map shown in FIG 2 with the final atomic surface structure overlaid. When refined against experimental data, in-plane atomic positions with a global temperature factor gave  $\chi^2 = 3.37$  and  $R_1 = 0.25$ . These numbers are slightly high, but with only 43 reflections, adding too many additional parameters is not justifiable even if it reduces the  $R_1$ . As a test, SHELXL [34] was used, and with the addition of anisotropic temperature factors,  $R_1$  decreased by 14%. This is suggestive of a rotation of the Ti atom located at the edge of surface unit cell (Ti3) which is consistent both with the EDM map (showing a streak at this site) as well as being the type of disorder expected if there are surface defects, and for the lowest-energy phonon mode (which will involve alternate rotations within a  $c(2 \times 2)$  supercell) (see supplemental material). For completeness, there was no indication of reduced occupancy of the Ti3 site. Since maps do not provide registry information and O sites are hard to determine from the maps alone, it was assumed that Ti atoms were bonded to O atoms in the layer immediately beneath the surface (subsurface layer), verified later by DFT.

The surface energies for RT13 along with other surfaces are plotted in FIG 3, with the convex-hull line marked indicating the lowest energy configurations as a function of excess TiO<sub>2</sub>. The RT13 fits in nicely with other solved surfaces, making it a feasible surface for 1.115 excess TiO<sub>2</sub> per bulk  $(1 \times 1)$ . Although the  $(\sqrt{2} \times \sqrt{2})R45^\circ$  (RT2) has the lowest energy for a surface with 1.5 excess TiO<sub>2</sub> per bulk  $(1 \times 1)$ , it has never been observed experimentally, unlike the higher energy  $c(4 \times 2)$  and  $(2 \times 2)$ , which are well documented, so we have used the latter for the convex hull.

The RT13 structure (FIG 4) has ten  $\text{TiO}_5$  polyhedra units that share edges with  $\text{TiO}_6$  octahedra located in the subsurface. There is also one  $\text{TiO}_5$  unit in the subsurface that remains corner-sharing with neighboring octahedra and is stabilized by rotations of the octahedra in the bulk beneath them. Ti-O bond distances in the surface  $\text{TiO}_5$  units are comparable to those in the bulk while, unsurprisingly, Ti-O bonds from surface Ti to subsurface O are slightly smaller than those in bulk (1.89 vs. 1.97 Å). The in-plane positions of surface atoms remained in excellent agreement with those found by EDM as well as having all surface bond-valence sums close to 2- for O and 4+ for Ti, as expected for a stable structure [2] (see supplemental material).

Worthy of note is that the surface can be considered as an ordered network of corner and edge-sharing  $\text{TiO}_5$  units, similar to other  $\text{SrTiO}_3$  (001) surfaces but now in a more open network. One can build an almost endless sequence of such structures by changing the number of each type of unit, both regularly to form an ordered reconstruction or semi-randomly to form a 2D glass. Beyond this, one can generate very similar structures as  $\text{TiO}_2$  single-layers, i.e. just on top of a SrO termination, or use combinations of the building blocks in other fashions. As an example, we have constructed and calculated a  $(3\times 3)$  structure (see supplemental material) which is consistent with experimental STM images [24] and close to the convex hull, as well as a  $(\sqrt{5}\times\sqrt{5})R26.6^\circ$  (RT5) reconstruction also within the convex hull.

Pulling together the arguments above about how these different structures can be generated by tiling of locally bond-valence satisfied units as well as the relatively small differences in the surface energies found from the DFT calculations, we believe a consistent picture is starting to emerge. Depending upon exact details of how the surfaces are prepared as well as local compositional inhomogeneities and the entropy of mixing, numerous structures can coexist locally, as well as disordered glass-like structures with only local order. With relatively sluggish surface diffusion kinetics these may persist for extended periods of time, only ordering after longer times than used in many experimental studies. We suspect that this type of disorder is common for perovskite oxide surfaces (and perhaps interfaces) and may be more general, similar to the Si-Au (111)  $(6\times 6)$  structure which has pentagonal units in a pseudo-glass structure [36, 37] shown recently to be related to a Au-Si eutectic liquid interface structure [38].

This work was funded by the DOE under Grant No DE-FG02-01ER45945.

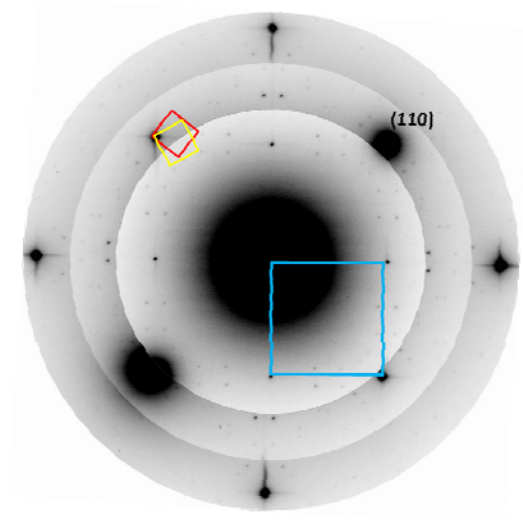


FIG 1 (Color online). Off-zone TEM diffraction pattern of RT13 with outlined bulk surface cell (blue) and two domains of RT13 (red, yellow).

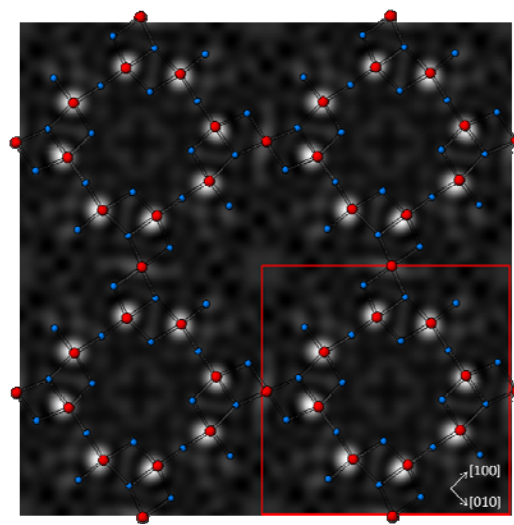


FIG 2 (Color online). Geometrically relaxed RT13 atomic surface layer overlaid scattering potential map solution obtained from EDM showing agreement with DFT structural results. One Ti is missing in the map which is not an unusual occurrence. Ti are larger (red), O are smaller (blue).

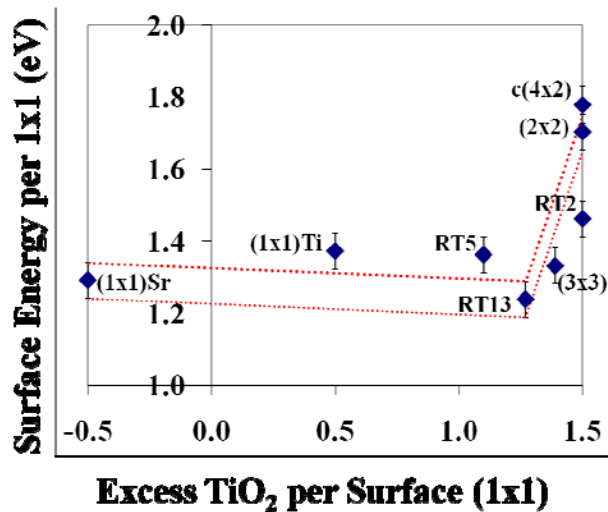


FIG 3 (Color online). Surface energies in eV per  $(1 \times 1)$  cell versus number of  $\text{TiO}_2$  units per  $\text{SrTiO}_3$   $(1 \times 1)$  surface unit cell for various  $\text{SrTiO}_3$   $(001)$  reconstructions. Region between dotted (red) lines shows convex-hull (including DFT error estimate) connecting the lowest energy surface pathway.  $\text{SrTiO}_3$   $(001)$  theoretical reconstructions, RT5 and  $(3 \times 3)$ , fall close to the convex hull.

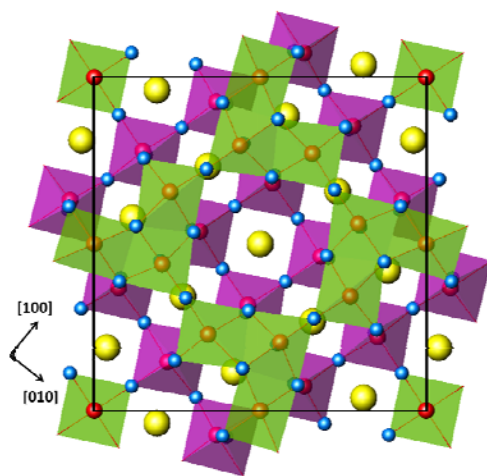


FIG 4 (Color online). Top view of RT13 with  $\text{TiO}_6$  octahedra (pink) and  $\text{TiO}_5$  polyhedra (green).  $\text{TiO}_5$  unit at the corner is in the subsurface layer. Ti (red), Sr (yellow), O (blue). For side view, see supplemental material.

1. A. N. Chiaramonti, C. H. Lanier, L. D. Marks and P. C. Stair, *Surf. Sci.* **602**, 3018 (2008).
2. J. A. Enterkin, *et. al.*, *Nat. Mater.* **9**, 245 (2010).
3. V. E. Henrich, G. Dresselhaus and H. J. Zeiger, *Phys. Rev. B* **17**, 4908 (1978).
4. M. R. Castell, *Surf. Sci.* **505**, 1 (2002).
5. J. E. T. Andersen and P. J. Möller, *Appl. Phys. Lett.* **56**, 1847 (1990).
6. P. A. W. van der Heide, Q. D. Jiang, Y. S. Kim and J. W. Rabalais, *Surf. Sci.* **473**, 59 (2001).
7. G. Charlton, *et. al.*, *Surf. Sci.* **457**, L376 (2000).
8. Q. D. Jiang and J. Zegenhagen, *Surf. Sci.* **338**, L882 (1995).
9. B. Cord and R. Courths, *Surf. Sci.* **162**, 34 (1985).
10. M. Kawasaki, *et. al.*, *Appl. Surf. Sci.* **107**, 102 (1996).
11. N. Erdman, *et. al.*, *J. Am. Chem. Soc.* **125**, 10050 (2003).
12. M. Naito and H. Sato, *Phys. C* **229**, 1 (1994).
13. N. Erdman, *et. al.*, *Nature* **419**, 55 (2002).
14. T. Matsumoto, *Surf. Sci.* **278**, L153 (1992).
15. P. J. Möller, S. A. Komolov and E. F. Lazneva, *Surf. Sci.* **425**, 15 (1999).
16. T. Kubo and H. Nozoye, *Surf. Sci.* **542**, 177 (2003).
17. J. Zegenhagen, T. Haage and Q. D. Jiang, *Appl. Phys. A* **67**, 711 (1998).
18. M. R. Castell, *Surf. Sci.* **516**, 33 (2002).
19. C. H. Lanier, *et. al.*, *Phys. Rev. B* **76**, 045241 (2007).
20. T. Kubo and H. Nozoye, *Phys. Rev. Lett.* **86**, 1801 (2001).
21. H. Tanaka, T. Matsumoto, T. Kawai and S. Kawai, *Jap. J. Appl. Phys.* **32**, 1405 (1993).
22. R. Akiyama, T. Matsumoto, H. Tanaka and T. Kawai, *Jap. J. Appl. Phys.* **36**, 3881 (1997).
23. M. S. M. Gonzalez, *et. al.*, *Solid State Sci.* **2**, 519 (2000).
24. D. T. Newell, Cambridge, 2007.
25. W. H. Zachariasen, *J. Chem. Soc.* **54**, 3841 (1932).
26. P. Xu, G. Jayaram and L. D. Marks, *Ultramicroscopy* **53**, 15 (1994).
27. R. Kilaas, L. D. Marks and C. S. Own, *Ultramicroscopy* **102**, 233 (2005).
28. P. Blaha, *et. al.*, *WIEN2k, An Augmented Plane Wave + Local Orbitals Program for Calculating Crystal Properties.* (Karlheinz Schwarz Techn., Universitat Wien, Austria, 2001).
29. J. P. Perdew, *et. al.*, *Phys. Rev. Lett.* **100**, 136406 (2008).
30. V. N. Staroverov, G. E. Scuseria, J. Tao and J. P. Perdew, *J. Chem. Phys.* **119**, 12129 (2003).
31. J. Ciston, A. Subramanian, D. M. Kienzle and L. D. Marks, *Surf. Sci.* **604**, 155 (2010).
32. L. D. Marks, A. N. Chiaramoniti, F. Tran and P. Blaha, *Surf. Sci.* **603**, 2179 (2009).
33. J. A. Enterkin, Northwestern University, 2010.
34. J. Fompeyrine, *et. al.*, *Appl. Phys. Lett.* **72**, 1697 (1998).
35. G. M. Sheldrick, *Acta Cryst.* **A64**, 112 (2008).
36. L. D. Marks, *et. al.*, *Surf. Rev. Lett.* **5**, 459 (1998).

37. D. Grozea, *et. al.*, Surf. Sci. **418**, 32 (1998).

38. T. U. Schulli, *et. al.*, Nature **464**, 1174 (2010).

See EPAPS Document No. [number will be inserted by publisher] for supplemental material. For more information on EPAPS, see <http://www.aip.org/pubservs/epaps.html>.